

Ligand and Counterion Control of Ag(I) Architectures: Assembly of a {Ag₈} Ring Cluster Mediated by Hydrophobic and Ag···Ag InteractionsJohn Fielden,^{†,§} De-liang Long,[†] Alexandra M. Z. Slawin,[‡] Paul Kögerler,[§] and Leroy Cronin^{*†}

WestCHEM, Department of Chemistry, University of Glasgow, Joseph Black Building, University Avenue, Glasgow G12 8QQ, United Kingdom, EastCHEM, School of Chemistry, University of St. Andrews, North Haugh, St. Andrews, Fife KY16 9ST, United Kingdom, and Ames Laboratory and Department of Physics and Astronomy, Iowa State University, Ames, Iowa 50011

Received May 6, 2007

A strategy combining ligand design and counterion variation has been used to investigate the assembly of silver(I) complexes. As a result, dinuclear, octanuclear, and polymeric silver(I) species have been synthesized by complexation of the rigid aliphatic amino ligands *cis*-3,5-diamino-*trans*-hydroxycyclohexane (DAHC), *cis*-3,5-diamino-*trans*-methoxycyclohexane (DAMC), and *cis*-3,5-diamino-*trans*-tert-butylidimethylsilyloxy-cyclohexane (DATC) with silver(I) triflate, nitrate, and perchlorate. The compositions of these aggregates, established by X-ray crystallography and elemental analysis, are [Ag(DAHC)]₂(CF₃SO₃)₂ (**1**), [Ag(DAMC)]₂(CF₃SO₃)₂ (**2**), [Ag(DAMC)]₂(NO₃)₂ (**3**), [Ag(DATC)]₆[Ag(DAHC)]₂(NO₃)₈ (**4**), and [Ag(DATC)]_n(NO₃)_n (**5**), where the DAHC present in **4** is formed by in situ hydrolysis of the acid labile silyl ether group. The type of aggregate formed depends both upon the noncoordinating O-substituent of the ligand and the (also noncoordinating) counterion, with the normal preference of the ligand topology for forming Ag₂L₂ structures being broken by introduction of the bulky, lipophilic O-*tert*-butylidimethylsilyl (TBDMS) group. Of particular note is the octanuclear silver ring structure **4**, which is isolated only when both the O-TBDMS group and the nitrate counteranion are present and is formed from four Ag₂L₂ dimers connected by Ag···Ag and hydrogen-bonding interactions. Diffusion rate measurement of this {Ag₈} complex by ¹H NMR (DOSY) indicates dissociation in CD₃OD and CD₃CN, showing that this supramolecular ring structure is formed upon crystallization, and establishing a qualitative limit to the strength of Ag···Ag interactions in solution. When solutions of the {Ag₈} cluster in methanol are kept for several days though, a new UV-vis absorption is observed at around 430 nm, consistent with the formation of silver nanoparticles.

Introduction

The controlled formation of metal–ligand complexes followed by their aggregation to oligomers, polymers, clusters, and networks is of great interest as a potential route to control primary, secondary, tertiary, and even quaternary interactions in the formation of materials with desired structure and function.¹ In particular, the ability to use both ligand design and adjustment of reaction conditions to understand and control the aggregation processes is vital, because the combination of these approaches should increase

the chance of designed synthesis of sophisticated, functional complexes and clusters.^{1–4} Thus, although rational design strategies have enjoyed considerable success in controlling structure by employing large, rigid ligands and metal centers with well-defined coordination preferences,⁵ the results of using smaller ligands and metals offering multiple coordination modes (e.g., copper(II) and silver(I)) are less predictable.^{1,6} In this case, the directing effects of the ligands are weaker and other variables, most notably the coordination,

* To whom correspondence should be addressed: E-mail: L.Cronin@chem.gla.ac.uk.

[†] WestCHEM, University of Glasgow.

[‡] EastCHEM, University of Glasgow.

[§] Iowa State University.

(1) Khlobystov, A. N.; Blake, A. J.; Champness, N. R.; Lemenovskii, D. A.; Majouga, A. G.; Zyk, N. V.; Schröder, M. *Coord. Chem. Rev.* **2001**, *222*, 155.

(2) Morgenstern, B.; Steinhäuser, S.; Hegetschweiler, K.; Garribba, E.; Micera, G.; Sanna, D.; Nagy, L. *Inorg. Chem.* **2004**, *43*, 3116.

(3) Applegarth, L.; Goeta, A. E.; Steed, J. W. *Chem. Commun.* **2005**, 2405.

(4) Turner, D. R.; Hursthouse, M. B.; Light, M. E.; Steed, J. W. *Chem. Commun.* **2004**, 1354.

(5) Fujita, M.; Umamoto, K.; Yoshizawa, M.; Fujita, N.; Kusukawa, T.; Biradha, K. *Chem. Commun.* **2001**, 509.

(6) Matthews, C. J.; Avery, K.; Xu, Z. Q.; Thompson, L. K.; Zhao, L.; Miller, D. O.; Biradha, K.; Poirier, K.; Zaworotko, M. J.; Wilson, C.; Goeta, A. E.; Howard, J. A. K. *Inorg. Chem.* **1999**, *38*, 5266.

hydrogen bonding, or templating abilities of the solvent or counterion, can significantly influence the outcome of the reaction.^{7,8} We hope that careful consideration of different coordination compounds formed in systematically varied conditions might gradually increase the understanding of these systems and allow a more rational approach in this field. Motivation for such work is provided by the properties of a wide variety of multinuclear coordination compounds, both designed and “discovered”, which have exhibited phenomena including catalysis of organic reactions⁹ and optical properties.^{10–12}

Silver(I) coordination compounds have attracted considerable interest in inorganic and supramolecular chemistry because of the coordinative flexibility of Ag(I):^{13–16} as well as linear, trigonal, tetrahedral, or octahedral coordination modes, Ag(I) centers can form Ag...Ag bonding interactions due to argentophilicity.¹⁷ Given this structural versatility (or unpredictability!), many examples of Ag(I) coordination polymers, nets,^{1,3} and discrete multinuclear complexes have been reported,^{10,18–23} including tri- and tetrameric silver clusters stabilized by *N*-heterocyclic carbenes²¹ and Ag...Ag-linked dimers of silver pyrazolate trimers.^{20,22} Furthermore, for a given Ag(I) system, a number of different structures might have similar energetic stabilities, allowing weak secondary noncovalent interactions to exert an unusually strong influence over the type of complex formed, as well-demonstrated by silver thiomethylterpyridine chemistry.²³ For this reason, silver(I) coordination compounds provide an excellent opportunity to investigate the effects of such weak interactions on structure. It should be noted that Ag...Ag interactions or bonds are frequently involved in such structures,^{13,17} yet their role and strength remains poorly understood. Suggested strengths range from below 5

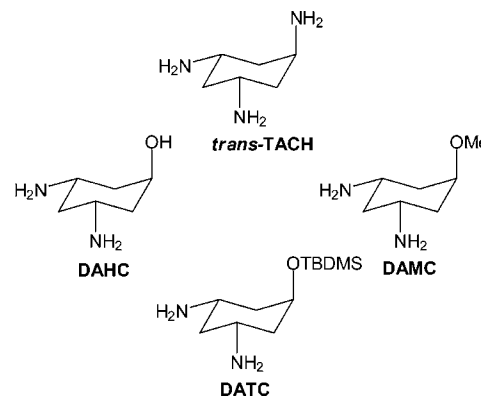


Figure 1. *trans*-TACH (top), DAHC and DAMC (middle), and DATC (bottom). The steric bulk and lipophilicity of the pendant “tail” O-substituent increases through the series DAHC to DATC.

kcal mol⁻¹,¹⁴ to a covalent bond order of approximately 1/3.¹⁵ This is partly because support from bridging metal–ligand bonds frequently complicates assessment of the structural significance of Ag...Ag bonding.¹⁶

Recent work in our group has focused on the use of rigid aliphatic amino ligands based on 6-membered rings to synthesize a range of interesting discrete and infinite silver(I) coordination complexes.^{24–27} These ligands, comprising *cis*-1,3,5-triaminocyclohexane (*cis*-TACH), *trans*-1,3,5-triaminocyclohexane (*trans*-TACH), *cis*-1,3-diaminocyclohexane (*cis*-DACH), and *cis*-1,3-diaminopiperidine (DAPI), all have a *cis*-1,3-diamino donor set, while variation of the atom, substituent or stereochemistry at the 5-position of the ring influences the exact shape and dimensionality of the complex. Subsequently, we have developed the heteroleptic, alcohol-substituted analogue *cis*-3,5-diamino-*trans*-hydroxy-cyclohexane (DAHC, Figure 1),²⁷ and described its copper coordination chemistry,^{28,29} along with that of the O-methyl derivative, *cis*-3,5-diamino-*trans*-methoxycyclohexane (DAMC), and the tetradentate glutaric acid derivative glutaric acid *bis*-(*cis*-3,5-diaminocyclohexyl) ester (GADACE).²⁹ Herein, we focus on the silver coordination chemistry of DAMC and the new ligand *cis*-3,5-diamino-*trans*-tert-butyldimethylsilyloxy-cyclohexane (DATC) (Figure 1), in which a combination of the counterion and the noncoordinating ligand O-substituent determine the nature of the complex formed. Complexation of silver(I) triflate or nitrate with DAMC or DAHC yields the dimeric complexes, $[\{Ag(DAMC)\}_2](NO_3)_2$ (**1**), $[\{Ag(DAHC)\}_2](CF_3SO_3)_2$ (**2**), and $[\{Ag(DAMC)\}_2](NO_3)_2$ (**3**), whereas DATC yields an octanuclear cluster, $[\{Ag(DATC)\}_6\{Ag(DAHC)\}_2](NO_3)_8$ (**4**), with silver(I) nitrate and a 1D polymer chain, $[\{Ag(DATC)\}_n](ClO_4)_n$ (**5**), with silver(I) perchlorate. Of particular note is the $\{Ag_8\}$ ring structure **4**, where four dimer subunits are connected by Ag...Ag interactions bridged only by hydrogen bonds.

- (7) Blake, A. J.; Brechin, E. K.; Codron, A.; Gould, R. O.; Grant, C. M.; Parsons, S.; Rawson, J. M.; Wimpenny, R. E. P. *J. Chem. Soc., Chem. Commun.* **1995**, 1983.
- (8) Murugesu, M.; Anson, C. E.; Powell, A. K. *Chem. Commun.* **2002**, 1054.
- (9) Yoshizawa, M.; Takeyama, Y.; Kusakawa, T.; Fujita, M. *Angew. Chem., Int. Ed.* **2002**, *41*, 1347.
- (10) Catalano, V. J.; Kur, H. M.; Garnas, J. *Angew. Chem., Int. Ed.* **1999**, *38*, 1979.
- (11) Han, L.; Yuan, D.; Xu, Y.; Wu, M.; Gong, Y.; Wu, B.; Hong, M. *Inorg. Chem. Commun.* **2005**, *8*, 529.
- (12) Galli, S.; Masciocchi, N.; Cariati, E.; Sironi, A.; Barea, E.; Haj, M. A.; Navarro, J. A. R.; Salas, J. M. *Chem. Mater.* **2005**, *17*, 4815.
- (13) A search of the Cambridge Structural Database (version 5.28, January 2007) found more than 717 structures containing Ag–Ag bonds.
- (14) Catalano, V. J.; Kur, H. M.; Garnas, J. *Angew. Chem., Int. Ed.* **1999**, *38*, 1979.
- (15) Baenziger, N. C.; Struss, A. W. *Inorg. Chem.* **1976**, *15*, 1807.
- (16) Amoroso, A. J.; Jeffrey, J. C.; Jones, P. L.; McCleverty, J. A.; Psillakis, E.; Ward, M. D. *J. Chem. Soc., Chem. Commun.* **1995**, 1173.
- (17) Pyykkö, P. *Chem. Rev.* **1997**, *97*, 597.
- (18) van Stein, G. C.; van der Poel, H.; van Koten, G.; Spek, A. L.; Duisenberg, A. J. M.; Pregosin, P. S. *J. Chem. Soc., Chem. Commun.* **1980**, 1016.
- (19) Eastland, G. W.; Mazid, M. A.; Russell, D. R.; Symons, M. C. R. *J. Chem. Soc., Dalton Trans.* **1980**, 1682.
- (20) Meyer, F.; Jacobi, A.; Zsolnai, L. *Chem. Ber.* **1997**, *130*, 1441; Reiss, P.; Fenske, D. *Z. Anorg. Allg. Chem.* **2000**, *626*, 2445.
- (21) Garrison, J. C.; Youngs, W. J. *Chem. Rev.* **2005**, *105*, 3978.
- (22) Dias, H. V. R.; Gamage, C. S. P.; Keltner, J.; Diyabalanage, H. V. K.; Omari, I.; Eyobo, E.; Dias, N. R.; Roehr, N.; McKinney, L.; Poth, T. *Inorg. Chem.* **2007**, *46*, 2979.
- (23) Hannon, M. J.; Painting, C. L.; Plummer, E. A.; Childs, L. J.; Alcock, N. W. *Chem.–Eur. J.* **2002**, *8*, 2225.

- (24) Pickering, A. L.; Seeber, G.; Long, D.-L.; Cronin, L. *Chem. Commun.* **2004**, 136.
- (25) Pickering, A. L.; Long, D.-L.; Cronin, L. *Inorg. Chem.* **2004**, *43*, 4953.
- (26) Seeber, G.; Pickering, A. L.; Long, D. L.; Cronin, L. *Chem. Commun.* **2003**, 2002.
- (27) Fielden, J.; Sprott, J.; Cronin, L. *New J. Chem.* **2005**, 1152.
- (28) Fielden, J.; Long, D.-L.; Cronin, L. *Chem. Commun.* **2004**, 12156.
- (29) Fielden, J.; Sprott, J.; Long, D.-L.; Kögerler, P.; Cronin, L. *Inorg. Chem.* **2006**, *45*, 2886.

The absence of bridging metal–ligand bonds opens possibilities to probe the strength and nature of the $\text{Ag}\cdots\text{Ag}$ bond in this structure.

Experimental Section

Materials, Methods, and Instrumentation. The ligands DAMC and DATC were synthesized starting from *cis*-1,3,5-cyclohexanetriol.²⁷ All other reagents and solvents were purchased as AR grade and used without further purification. Deuterated solvents were obtained from Aldrich. All complexations were performed in the ambient atmosphere. Infrared spectra were measured with a Jasco FTIR-410 spectrometer, UV–vis spectra with a Shimadzu UV-1601PC spectrophotometer, ¹H NMR measurements were performed using Bruker DPX-400, Avance-400, and DRX-400 spectrometers, and electrospray mass spectra were recorded with a Applied Biosystems QStar Pulsar i spectrometer. X-ray diffraction data were collected using a Nonius Kappa-CCD diffractometer with Mo–K α radiation and a graphite monochromator (compounds **1–3**, **5**) and using a MM-007/VariMax-Mo/Mercury CCD with Mo–K α radiation and a graphite monochromator (compound **4**). The supplementary data for the structures of compounds **1–5** is given in the associated CIF files. DFT calculations were performed using triple- ζ valence basis sets with augmented polarization functions, and hybrid B3-LYP exchange and correlation functionals.

Preparation of $[\{\text{Ag}(\text{DAHC})\}_2](\text{CF}_3\text{SO}_3)_2$ (1**).** Silver(I) triflate (0.099 g, 0.385 mmol) in methanol (2 mL) was added to DAHC (0.050 g, 0.384 mmol) in methanol (20 mL) and the colorless mixture was stirred in the dark for 90 min. The volume was subsequently reduced to ca. 2 mL and the title compound isolated as colorless crystals (0.0184 g, 0.0228 mmol, 12%) by diffusion of diethyl ether into the methanolic solution over 10 days in the dark. ¹H NMR (400 MHz, CD₃OD): δ 4.41 (m, 2H), 3.29 (tt, 4H), 2.31 (broad d, 2H), 2.00 (broad d, 4H), 1.15 (broad pt, 4H), 1.10 (pq, 2H). IR (KBr disc) cm⁻¹: 3477 m, 3170 w, 2926 m, 2853 w, 1598 m, 1459 w, 1385 w, 1255 vs, 1174 s, 1032 s, 981 w, 828 w, 759 w, 703 w, 642 s. Elemental anal. Calcd for C₁₄H₂₈Ag₂F₆N₄O₈S₂ (**1**): C, 21.72; H, 3.65; N, 7.24. Found: C, 21.83; H, 3.66; N, 7.14.

Preparation of $[\{\text{Ag}(\text{DAMC})\}_2](\text{CF}_3\text{SO}_3)_2$ (2**).** Silver(I) triflate (0.0899 g, 0.35 mmol) in methanol (2 mL) was added to DAMC (0.05 g, 0.35 mmol) in methanol (20 mL) and the colorless mixture was stirred in the dark for 2 h. The volume was reduced to ca. 5 mL, and after filtration, the clear solution was crystallized by diffusion of diethyl ether, yielding the colorless title compound (0.0165 g, 0.0198 mmol, 11%). ¹H NMR (400 MHz, CD₃OD): δ 3.64 (m, 2H), 3.22 (s, solvent + 6H), 3.14 (tt, 4H), 2.28 (dt, 2H), 2.17 (broad d, 4H), 1.17–1.03 (m, 6H). ES⁺-MS: *m/z* 2458.2 [Ag₁₃L₁₃(OTf)₁₁]²⁺, 2386.2 [Ag₁₃L₁₂(OTf)₁₁]²⁺, 2257.2 [Ag₆L₆(OTf)₅]⁺, 2113.0 [Ag₆L₅(OTf)₅]⁺, etc. (low intensity), 653.0 [Ag₂L₂(OTf)]⁺ (high intensity). IR (diamond anvil) cm⁻¹: 3502 w, 3256 m, 2902 w, 1592 m, 1454 m, 1237 s, 1221 s, 1154 s, 1071 m, 1022 s. Elemental anal. Calcd for C₁₆H₃₂Ag₂F₆N₄O₈S₂ (**2**): C, 23.95; H, 4.02; N, 6.98. Found: C, 23.94; H, 4.23; N, 6.52.

Preparation of $[\{\text{Ag}(\text{DAMC})\}_2](\text{NO}_3)_2$ (3**).** Silver(I) nitrate (0.0295 g, 0.173 mmol) in methanol (1 mL) was added to DAMC (0.025 g, 0.173 mmol) in methanol (3 mL) and the colorless mixture was stirred in the dark for ca. 3 h. The resulting clear solution was set to crystallize by ether diffusion (slowed by cooling in the refrigerator), yielding colorless crystals of the title compound (0.022 g, 0.035 mmol, 40.4%). ¹H NMR (400 MHz, CD₃OD): δ 3.64 (m, 2H), 3.22 (s, 6H), 3.21 (tt, 4H), 2.30 (broad d, 2H), 2.17 (broad d, 4H), 1.20–1.03 (m, 6H). IR (diamond anvil) cm⁻¹: 3430 w, 3290 m, 3154 w, 2929 m, 1603 m, 1461 w, 1355 s, 1187 w, 1150 s,

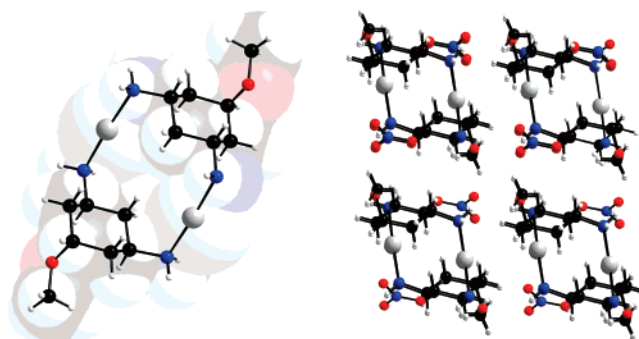


Figure 2. $[\{\text{Ag}(\text{DAMC})\}_2]^{2+}$ complex cation observed in compounds **2** and **3**. The complex cation of **1** is isostructural with OH replacing the OMe tail group. Carbon is black; O, red; N, blue; Ag, gray; color scheme retained in all.

1078 s, 953 w, 812 w. UV–vis (MeOH) nm: 302.5. Elemental anal. Calcd for C₁₄H₃₂Ag₂N₆O₈: C, 26.77; H, 5.13; N, 13.38. Found: C, 26.71; H, 5.11; N, 13.15.

Preparation of $[\{\text{Ag}(\text{DATC})\}_6\{\text{Ag}(\text{DAHC})\}_2(\text{NO}_3)_8$ (4**).** Silver(I) nitrate (0.035 g, 0.206 mmol) in a small quantity of methanol was added to a solution of DATC (0.050 g, 0.205 mmol) in methanol (20 mL). After being stirred in darkness for ca. 4 h, the clear, colorless solution was reduced in volume to ca. 2.5 mL on a rotary evaporator before filtration and crystallization in darkness by ether diffusion yielded the title compound as clear colorless crystals (0.0157 g, 18.5%) in 5–7 days. ¹H NMR (400 MHz, CD₃OD): δ 4.22 (m, 1H), 3.30 (*ptpt*, 2H), 2.32 (m, 1H), 1.94 (m, 2H), 1.16 (*pt*, 2H), 1.10 (*pq*, 1H), 0.81 (s, 9H), 0.00 (s, 6H). ES⁺-MS showed oligomers: *m/z* 1887.2 [Ag₁₀L₉(NO₃)₉], 1765.1 [Ag₁₀L₈(NO₃)₈]²⁺, 1680.1 [Ag₉L₈(NO₃)₇]²⁺, 1473.4 [Ag₈L₇(NO₃)₆]²⁺, 1350.3 [Ag₄L₃(NO₃)₃]⁺, etc. (low intensity); 776.0 [Ag₂L₂(NO₃)]⁺, 595.3 [AgL]⁺, 351.1 [AgL]⁺ (high intensity). IR (KBr disc) cm⁻¹: 3282 s, 3153 w, 2927 m, 2855 m, 1605 m, 1384 s, 1256 m, 1063 m, 826 m. UV–vis (MeOH) nm: 300.5. Elemental anal. Calcd for $[\{\text{Ag}(\text{DATC})\}_6\{\text{Ag}(\text{DAHC})\}_2](\text{NO}_3)_8 \cdot 8\text{H}_2\text{O} = \text{C}_{84}\text{H}_{212}\text{Ag}_8\text{N}_{24}\text{O}_{40}\text{Si}_6$ (**4**·8H₂O): C, 31.23; H, 6.62; N, 10.41. Found: C, 31.69; H, 6.17; N, 10.55.

Preparation of $[\{\text{Ag}(\text{DATC})\}_n](\text{ClO}_4)_n$ (5**).** Silver(I) perchlorate (0.0212 g, 0.102 mmol) in methanol (ca. 3 mL) was added to a methanolic solution (10 mL) of DATC (0.025 g, 0.103 mmol). **Caution:** perchlorates can be explosive. After the solution was stirred in the dark for 3 h, the volume was reduced in vacuo to ca. 1.5 mL before the title compound was crystallized as small, colorless rectangles by ether diffusion (0.0195 g, 42%). ¹H NMR (400 MHz, CD₃OD): δ 4.23 (m, 1H), 3.32 (m, 2H), 2.32 (m, 1H), 1.95 (m, 2H), 1.17 (m, 3H), 0.81 (s, 9H), 0.00 (s, 6H). IR (KBr disc) cm⁻¹: 3433 s, 3336 m, 3274 m, 2927 m, 2854 m, 1589 m, 1466 w, 1384 m, 1362 w, 1253 s, 902 m, 846 m, 779 m, 690 w. Elemental anal. Calcd for C₁₂H₃₀AgClN₂O₆Si (5·H₂O): C, 30.68; H, 6.44; N, 5.96. Found: C, 30.22; H, 5.88; N, 6.54.

Single-Crystal Structure Determination. Suitable single crystals of **1–5** were mounted on the end of a thin glass fiber using Fomblin oil. X-ray diffraction intensity data for **1–3** and **5** were measured at 150 K on a Nonius Kappa-CCD diffractometer (λ (Mo–K α) = 0.7107 Å), whereas **4** was measured at 180 K on an MM-007/VariMax-Mo/Mercury CCD (λ (Mo–K α) = 0.7107 Å). Structure solution and refinement was carried out with SHELXS-97³⁰ and SHELXL-97³¹ via WinGX.³² Corrections for incident and

(30) Sheldrick, G. M. *Acta Crystallogr., Sect. A* **1998**, *46*, 467.

(31) *Programs for Crystal Structure Analysis*, release 97-2; Institut für Anorganische Chemie der Universität Göttingen: Göttingen, Germany, 1998.

Table 1. Crystallographic Data for **1–5**

| | 1 | 2 | 3 | 4 | 5 |
|--|---|--|--|---|---|
| empirical formula | C ₁₄ H ₂₈ Ag ₂ F ₆ N ₄ O ₈ S ₂ ·CH ₃ OH | C ₁₆ H ₃₂ Ag ₂ F ₆ N ₄ O ₈ S·1CH ₃ OH | C ₇ H ₁₆ AgN ₃ O ₄ | C ₈₄ H ₁₉₆ Ag ₈ N ₂₄ O ₃₂ Si ₆ ·8H ₂ O | C ₁₂ H ₂₈ AgClN ₂ O ₅ Si·H ₂ O |
| fw (g mol ⁻¹) | 806.31 | 834.36 | 314.10 | 3230.28 | 451.77 |
| cryst syst | orthorhombic | triclinic | triclinic | triclinic | monoclinic |
| <i>a</i> (Å) | 16.4817(7) | 10.6679(4) | 7.3623(3) | 14.3141(3) | 7.0267(3) |
| <i>b</i> (Å) | 7.8604(2) | 12.3778(6) | 8.7919(6) | 14.3913(3) | 9.6235(7) |
| <i>c</i> (Å) | 21.8412(9) | 12.6385(3) | 8.8932(6) | 37.9501(9) | 13.8161(9) |
| α (deg) | 90 | 101.404(2) | 111.832(3) | 90.172(2) | 90 |
| β (deg) | 90 | 113.443(2) | 99.411(3) | 100.697(2) | 91.824(4) |
| γ (deg) | 90 | 94.570(2) | 91.128(4) | 95.281(2) | 90 |
| space group | <i>Pca</i> 2 ₁ | <i>P</i> ₁ | <i>P</i> ₁ | <i>P</i> ₁ | <i>P</i> 2 ₁ |
| <i>V</i> (Å ³) | 2829.59(18) | 1477.43(10) | 525.13(5) | 7647.6(3) | 933.79(10) |
| <i>Z</i> | 4 | 2 | 2 | 2 | 2 |
| ρ _{calcd} (g cm ⁻³) | 1.893 | 1.876 | 1.986 | 1.403 | 1.607 |
| σ (mm ⁻¹) | 1.620 | 1.554 | 1.919 | 1.120 | 1.308 |
| <i>T</i> (K) | 150(2) | 150(2) | 150(2) | 180(2) | 150(2) |
| no. of observations (unique) | 16155 (4743) | 20134 (5799) | 7065 (1856) | 43040 (19252) | 4675 (1948) |
| residuals: <i>R</i> ; <i>R</i> _w ^a | 0.062; 0.160 | 0.037; 0.078 | 0.082; 0.234 | 0.128; 0.331 | 0.036; 0.072 |

$$^a R_1 = \sum ||F_o| - |F_c|| / \sum |F_o|. \quad wR_2 = \{ \sum [w(F_o^2 - F_c^2)^2] / \sum [w(F_o^2)^2] \}^{1/2}.$$

Table 2. Silver–Nitrogen Bond Lengths (Å) and Angles (deg) in Complexes **1–3**

| 1 | | 2 | | 3 | |
|-----------------|-------------|-----------------|-------------|--------------|-------------|
| bond | length (Å) | bond | length (Å) | bond | length (Å) |
| Ag(1)–N(1) | 2.142(8) | Ag(1)–N(1) | 2.124(3) | Ag–N(1) | 2.174(14) |
| Ag(1)–N(3) | 2.136(8) | Ag(1)–N(2) | 2.129(3) | Ag–N(2) | 2.108(15) |
| Ag(2)–N(2) | 2.157(7) | Ag(2)–N(3) | 2.154(3) | | |
| Ag(2)–N(4) | 2.132(8) | Ag(2)–N(4) | 2.148(4) | | |
| bonds | angle (deg) | bonds | angle (deg) | bonds | angle (deg) |
| N(3)–Ag(1)–N(1) | 170.9(3) | N(1)–Ag(1)–N(2) | 176.56(13) | N(2)–Ag–N(1) | 175.6(5) |
| N(4)–Ag(2)–N(2) | 171.6(3) | N(4)–Ag(2)–N(3) | 175.10(13) | | |

diffracted beam absorption effects were applied using empirical³³ or numerical methods.³⁴ Compound **1** crystallized in the space group *Pca*2₁, **2–4** in *P*₁; and compound **5** in *P*2₁. All structures were solved by a combination of direct methods and difference Fourier syntheses and refined against *F*² by the full-matrix least-squares technique. Crystal data, data collection parameters, and refinement statistics for **1–3** are listed in Table 1.

Results and Discussion

Ligand Design Overview. This study utilizes ligands that are based on a rigid 1,3,5-functionalized cyclohexane backbone containing a *cis*-1,3-diamino moiety. Our previous studies showed that when the *trans* moiety is an amino group, as for the ligand *cis,trans*-1,3,5-triaminocyclohexane (*trans*-TACH), a great deal of versatility can result because the *cis*-diamine group can be used to coordinate to a metal ion or ions, and the *trans*-group can be protonated and anchor the unit in a hydrogen-bonded network.³⁵ By changing the *trans*-group to hydroxy, then methoxy, and finally the very bulky and lipophilic O–TBDMS, we have been able to investigate the influence of *trans*-groups with lower hydrogen bonding ability, and progressively greater steric demand and lipophilicity. (Figure 1).

Dimeric Complexes 1–3. Complexation of DAHC or DAMC with one equivalent of silver(I) triflate in methanol,

followed by ether diffusion, resulted in the crystallization of simple dimeric [{AgL₂}(OTf)₂] (L = DAHC, **1**; L = DAMC, **2**) structures in low (ca. 12%) yields. Use of DAMC with silver(I) nitrate resulted in more efficient crystallization, giving [{Ag(DAMC)}₂](NO₃)₂ (**3**) in a 40% yield; however, the same anion with DAHC instead caused rapid precipitation of microcrystalline material. In these complexes, which are essentially isostructural, two ligands are found in the *bis*-equatorial, *mono*-axial conformation and are linked into a dimer by two silver centers in a linear coordination mode (Figure 2). Silver–nitrogen bond lengths and angles are comparable in the three complexes, but the two DAMC-based structures (**2** and **3**) have N–Ag–N bond angles closer to the idealized 180° for 2-coordinate silver (Table 2). This may be a result of the non-hydrogen-bonding O–methyl tail group, which reduces the interaction of the complex cation with the network, hence decreasing the ability of hydrogen bonds to distort the metal coordination sphere.

The two triflate-based structures both include one methanol molecule and pack in extended hydrogen bonded arrays, which show two orientations for the complex cations; these are symmetry related in **1**, whereas in **2**, there are two crystallographically independent positions. However, in **1**, the cations are simply assembled into chains by the triflate anions, which provide hydrogen-bonded bridges between the alcohol groups (D···A distances ~2.85 Å) of one cation and the nitrogens (~3.05 Å) of the next. The included methanol molecule is shared between two 50% occupied positions and hydrogen bonds to triflate oxygens (~2.80 and 2.90 Å) on

(32) Farrugia, L. J. *J. Appl. Crystallogr.* **1999**, *32*, 837.

(33) Blessing, R. H. *Acta Crystallogr., Sect. A* **1995**, *51*, 33.

(34) Coppens, P.; Leiserowitz, L.; Rabinovich, D. *Acta Crystallogr., Sect. A* **1965**, *18*, 1035.

(35) Seeber, G.; Kögerler, P.; Kariuki, B. M.; Cronin, L. *Chem. Commun.* **2004**, 1580.

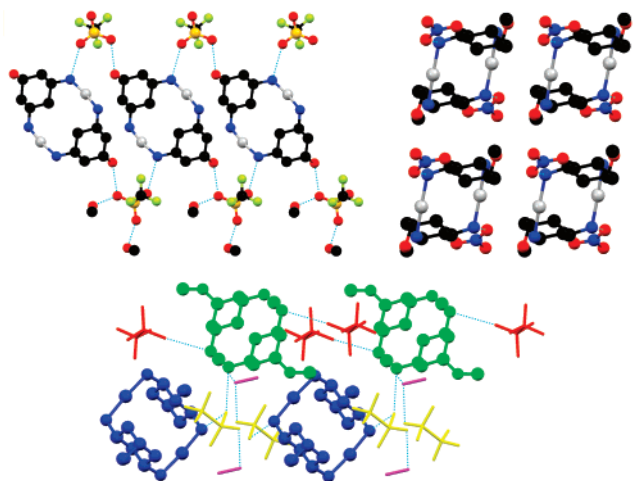


Figure 3. Crystal packing/hydrogen bonding in **1**·MeOH (top, left), **2**·MeOH (bottom) and **3** (top, right). **1** and **3** are viewed along the crystallographic *c*-axis; in **2**, the view is selected for clarity. Colors as in Figure 1 with S atoms orange; F, yellow. Compound **2** colored by symmetry equivalence with cations in blue/green, triflates in yellow/red, and MeOH purple. Hydrogen bonds are shown as bright blue dotted lines between donor/acceptor positions.

one side of the chain (Figure 3). In **2**, the “switching off” of the hydrogen bond donating alcohol tail group results instead in the formation of a 2D hydrogen-bonded network, where complex cations donate hydrogen bonds exclusively through their amine groups. Cations in the two positions are linked by hydrogen bonds via bridging triflate anions (~ 2.99 and 3.04 Å) and methanol molecules (~ 2.98 Å), which connect to the bridging triflates (~ 2.93 Å). The second triflate position is terminal, connecting to only one cation amine group (~ 3.04 Å). In nitrate-based structure **3**, the complex cations are assembled in a simple three-dimensional array, with the nitrate anions each accepting a hydrogen bond (~ 3.02 Å) from the amine of one cation. Formally, hydrogen bonds do not connect the cations into a network, as other $D\cdots A$ distances are greater than the sum of the Van der Waal radii.

Octameric Complex 4. Changing the ligand to DATC, with the bulkier, highly lipophilic *tert*-butyldimethylsilyl (TBDMS) tail group, has a dramatic effect on the outcome of the complexation reaction. A similar dimer unit forms, but these dimers crystallize (yield, 19%) to form the cyclic $\{Ag_8\}$ structure **4** (Figure 4), in which the dimers are connected by $Ag\cdots Ag$ bonding interactions. This $\{Ag_8\}$ ring is interesting in that it is the largest member of a rare class of cyclic cluster where $Ag\cdots Ag$ bonds play a structural role without being bridged (e.g., supported) by metal–ligand coordinate bonds. Previously isolated examples of this type comprise one $\{Ag_3\}$ ¹⁹ and two $\{Ag_6\}$ ²⁰ aggregates. As such, the $\{Ag_8\}$ aggregate provides an ideal opportunity to probe the strength of $Ag\cdots Ag$ bonds. Furthermore, by comparison with structures **3** and **5**, it illustrates the powerful influence of the counterion and “innocent” tail group over supramolecular architecture in this system; $\{Ag_8\}$ is only formed when both the TBDMS tail group and the nitrate anion are present.

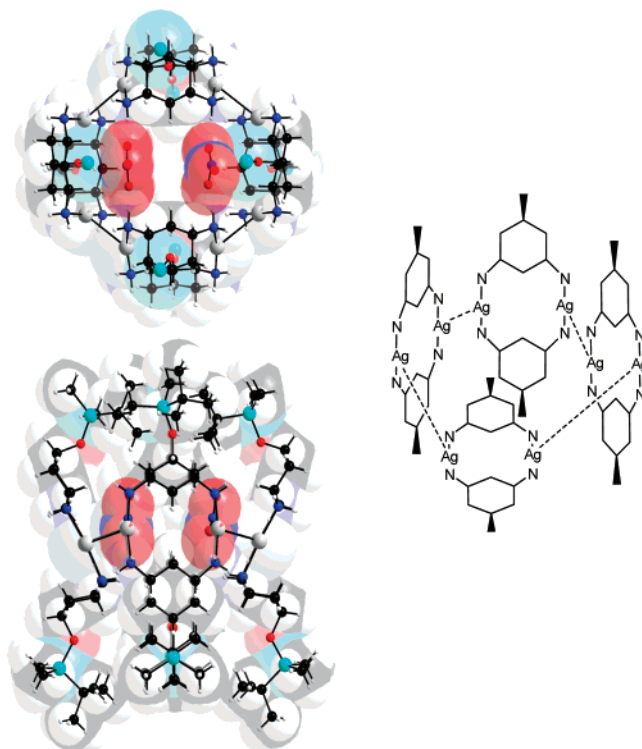


Figure 4. Complex cation in $[\{Ag(DATC)\}_6\{Ag(DAHC)\}_2(NO_3)_8]$, **4**, showing both the top view (top) and a side view (bottom). Both views show encapsulation of nitrate anions (space-filling). The encapsulated two methanol molecules are omitted for clarity. Color scheme as before and Si atoms cyan.

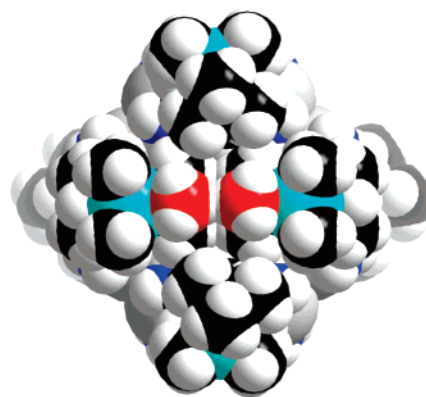


Figure 5. Space-filling representation of $[\{Ag(DATC)\}_6\{Ag(DAHC)\}_2(NO_3)_8]$, **4**, from the top compressed end. The two methyl groups would be clashing if their occupation was 100% are (C \cdots C distance of 3.157 Å) are shown in red.

Compound **4** has been characterized by X-ray diffraction, elemental analysis, FTIR, UV–vis, ES-MS, and ¹H NMR experiments including DOSY (see the Supporting Information).³⁶ Although the *R*-factor obtained for the crystal structure is rather high, it can be explained by the fact that the main body of the complex is formulated as $[\{Ag(DATC)\}_6\{Ag(DAHC)\}_2]$, where the DATC and the DAHC ligands differ in terms of OH or OTBDMS tail groups, which means that 25% of the eight tails are occupied with OH rather than OTBDMS. Therefore, the eight tail positions are disordered; however, the main body of the cluster is very well-defined, although four of the eight silver ions (Ag_1 ,

(36) Johnson, C. S., Jr. *Prog. NMR Spectrosc.* **1999**, *34*, 203.

Table 3. Silver Coordination Bonds and Angles in Compound **4**

| bond distances (Å) | | | | bond angles (deg) | | | |
|--------------------|------------|-------------|------------|-------------------|-------------|-------------------|-------------|
| Ag–N | | Ag···Ag | | N–Ag–N | | N–Ag···Ag | |
| bond | length (Å) | bond | length (Å) | bond | angle (deg) | bond | angle (deg) |
| Ag(1)–N(3) | 2.05(2) | Ag(1)–Ag(2) | 3.025(9) | N(3)–Ag(1)–N(1) | 168.1(8) | N(3)–Ag(1)–Ag(2) | 88.3(5) |
| Ag(1)–N(1) | 2.207(19) | Ag(3)–Ag(4) | 3.037(9) | N(6)–Ag(2)–N(8) | 175.1(7) | N(1)–Ag(1)–Ag(2) | 103.1(5) |
| Ag(2)–N(6) | 2.097(18) | Ag(5)–Ag(6) | 3.016(7) | N(5)–Ag(3)–N(7) | 173.8(6) | N(6)–Ag(2)–Ag(1) | 81.4(5) |
| Ag(2)–N(8) | 2.115(18) | Ag(7)–Ag(8) | 3.019(8) | N(12)–Ag(4)–N(10) | 168.1(9) | N(8)–Ag(2)–Ag(1) | 103.4(5) |
| Ag(3)–N(5) | 2.126(17) | | | N(11)–Ag(5)–N(9) | 167.8(7) | N(5)–Ag(3)–Ag(4) | 81.8(4) |
| Ag(3)–N(7) | 2.134(16) | | | N(16)–Ag(6)–N(14) | 173.7(6) | N(7)–Ag(3)–Ag(4) | 104.3(5) |
| Ag(4)–N(12) | 2.07(2) | | | N(15)–Ag(7)–N(13) | 173.5(6) | N(12)–Ag(4)–Ag(3) | 89.6(6) |
| Ag(4)–N(10) | 2.203(18) | | | N(4)–Ag(8)–N(2) | 167.2(7) | N(10)–Ag(4)–Ag(3) | 102.2(5) |
| Ag(5)–N(11) | 2.110(18) | | | | | N(11)–Ag(5)–Ag(6) | 91.7(5) |
| Ag(5)–N(9) | 2.221(18) | | | | | N(9)–Ag(5)–Ag(6) | 100.5(4) |
| Ag(6)–N(16) | 2.142(18) | | | | | N(16)–Ag(6)–Ag(5) | 100.1(5) |
| Ag(6)–N(14) | 2.143(18) | | | | | N(14)–Ag(6)–Ag(5) | 85.9(4) |
| Ag(7)–N(15) | 2.142(16) | | | | | N(15)–Ag(7)–Ag(8) | 100.7(5) |
| Ag(7)–N(13) | 2.146(17) | | | | | N(13)–Ag(7)–Ag(8) | 85.5(5) |
| Ag(8)–N(4) | 2.10(2) | | | | | N(4)–Ag(8)–Ag(7) | 90.8(5) |
| Ag(8)–N(2) | 2.255(19) | | | | | N(2)–Ag(8)–Ag(7) | 102.0(5) |

Ag4, Ag5, Ag8) have rather high thermal parameters, which was best treated by modeling them as being slightly disordered over two positions. Evidence for this hydrolysis is provided by a crystal structure showing only partial occupation (30–50%) of certain TBDMS C and Si positions, and elemental analysis (after drying under vacuum) consistent with the formula $\{[\text{Ag}(\text{DATC})]_6\{[\text{Ag}(\text{DAHC})]_2\}(\text{NO}_3)_8\} \cdot 8\text{H}_2\text{O}$. TBDMS ethers are well-known to be acid labile, and can be rapidly hydrolyzed in relatively mild conditions such as pyridinium *p*-toluenesulfonate in ethanol at room temperature.³⁷ Therefore, the use of a Lewis acidic silver(I) salt coupled with the presence of a certain quantity of water in the methanol could certainly have encouraged a degree of hydrolysis. Importantly, the partial hydrolysis of the ligand appears to be vital to formation of the $\{\text{Ag}_8\}$ cluster. It can be seen that TBDMS tail groups at one end of the cluster are highly disordered and two of the groups can only be reasonably modeled with an occupancy factor of ca. 50%. This low occupation is due to the fact that it would be impossible to accommodate the TBDMS groups in this space, as indicated by the very close interaction between two $-\text{CH}_3$ sites with a $\text{C}\cdots\text{C}$ distance of 3.157 Å. Therefore, this analysis allows us to confidently postulate that $\{[\text{Ag}(\text{DATC})]_6\{[\text{Ag}(\text{DAHC})]_2\}(\text{NO}_3)_8\}$ is the intrinsically stable product and that $\{[\text{Ag}(\text{DATC})]_8\}(\text{NO}_3)_8$ cannot form because of steric reasons, see Figure 5 Overall, the $\{\text{Ag}_8\}$ complex cation in **4** can be seen as having a metal–organic “calixarene” structure, an analogy supported by the location of two nitrate counterions, two methanol molecules, and other disordered atoms (water/methanol) inside the cavity of the ring. This cavity has minimum internal dimensions of approximately $4.54 \times 6.03 \times 10.04 \text{ \AA}^3$ (measured $\text{H}\cdots\text{H}$; i.e., an approximate volume of 0.25 nm^3), with cyclohexane rings as walls and TBDMS groups positioned around the entrance in a fashion reminiscent of the *tert*-butyl groups seen in classical calixarenes.³⁸ The silver centers have an approximately T-shaped coordination geometry, with a mean

bond length to nitrogen of 2.141(18) Å, although there is considerable variation within a range of 2.05(2)–2.255(19) Å (Table 3).

Silver–silver bond lengths average 3.024(8) Å, comparable to the median value of 3.00 Å found in the CSD.²⁵ DFT calculations (TZVP/B3-LYP) indicate significant overlap between silver orbitals and a Mulliken bond order of ca. 1/2.³⁹ Bond angles indicate slight distortion from an ideal T-shaped coordination sphere, with a mean N–Ag–N angle of 170.9(8)°, whereas twisting of the dimer units relative to each other around the Ag···Ag axes results in small and large N–Ag···Ag angles with mean values of 86.9(5) and 102.0(5)°, respectively (Table 3).

Inside the cavity, short contacts exist between the nitrate oxygen and the amine nitrogen atoms (2.92 Å) of the complex cation, which suggest a hydrogen-bonded interactions, while further hydrogen bonds occur between the nitrates and methanol molecules ($\text{D}\cdots\text{A}$ distances ≈ 2.44 , 2.48 Å). Externally, hydrogen bonds between the amine groups and nitrate anions bridge the silver–silver interactions, helping stabilize the structure ($\text{D}\cdots\text{A}$ distances range from 2.901 to 3.087 Å). Nitrate anions also allow the association of the complex cations into hydrogen-bonded layers, which run parallel to the crystallographic *ac* plane (Figure 6). It appears that between the layers there are hydrophobic contacts between the TBDMS tail groups.

The relative strength of Ag···Ag interaction suggested by DFT calculations, combined with the calixarene like structure of the $\{\text{Ag}_8\}$ cation, encouraged investigation of the solution chemistry of **4**. Furthermore, the Ag···Ag interactions in this compound are supported only by bridging hydrogen-bonded anions, which would be expected to dissociate upon dissolution; this gives us an opportunity to investigate the nature of the Ag···Ag bonds, which, although often considered to be extremely weak,¹⁷ have also been seen to maintain a multinuclear structure upon dissolution in toluene.²⁰ However, UV–vis measurements performed on **4** in both methanol and acetonitrile reveal an identical spectrum to the

(37) Greene, T. W.; Wuts, P. G. M. *Protective Groups in Organic Synthesis*, 2nd ed.; John Wiley & Sons, New York, 1991.

(38) Barea, E.; Navarro, J. A. R.; Salas, J. M.; Quirós, M. J.; Willermann, M.; Lippert, B. *Chem.—Eur. J.* **2003**, *9*, 4414.

(39) Single-molecule DFT calculations on an optimized geometry of $\{\text{Ag}_3\}$ were performed using the TURBOMOLE 5.7 program.

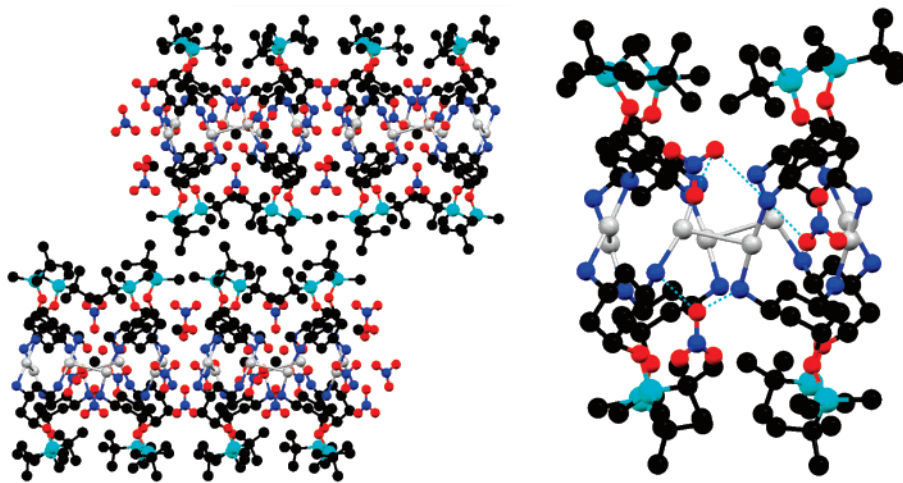


Figure 6. $[\{Ag(DATC)\}_6\{Ag(DAHC)\}_2(NO_3)_8]$ (**4**). Left: Crystal packing viewed along the crystallographic a -axis. Hydrogens and disordered tail group atoms have been omitted for clarity. Right: Hydrogen-bonded nitrate anions bridging the $Ag\cdots Ag$ interaction. Hydrogens, encapsulated molecules, and disordered atoms are omitted for clarity; hydrogen bonds are shown as bright blue dotted lines between donor/acceptor positions.

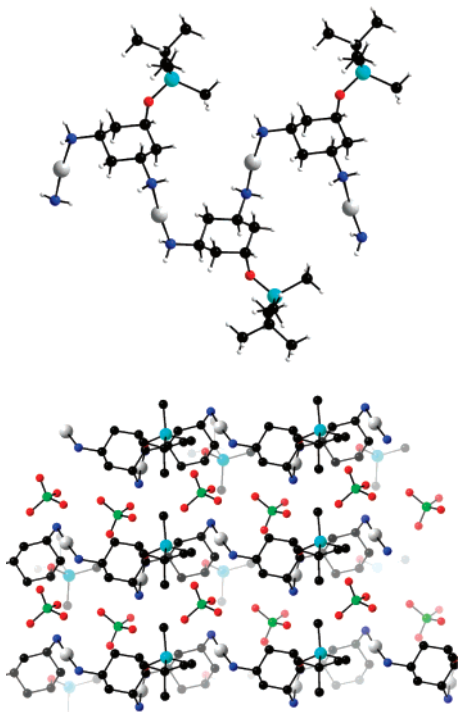


Figure 7. $[\{Ag(DAHC)\}_n](ClO_4)_n$, **5**. Top, side view of the polymer polycation; bottom, packing of the polymer strands with the perchlorate anion forming a layered structure. Color scheme as before, with Cl atoms in green.

isolated dimer **3**, suggesting the same silver coordination sphere and hence dissociation of the aggregate. This was supported by measurement of the diffusion rate of **4** by DOSY 1H NMR (CD_3OD and CD_3CN), which corresponded to a molecular weight of around 335 Daltons, consistent with dissociation of the complex into $[Ag(DATC)]^+$ cations, and ES^+ -MS showing strong peaks for Ag_2L_2 and smaller species, but much weaker peaks at higher m/z values. Notably, some peaks corresponding to large aggregates were also observed when the same techniques were applied to the simple dimer **2**. For both compounds, the observed isotope patterns were in good agreement with calculations, while the peak spacing (0.5 amu for 2^+ or 1 amu for 1^+) allowed assignment of the

aggregate charge. These results indicate that the $Ag\cdots Ag$ bonds are not stable in polar solvents, probably because of competition from transient coordination of solvent molecules to the $Ag(I)$ centers. Unfortunately, insolubility in less polar media prevented direct comparison with the literary measurements in toluene.²⁰ In addition, the NMR and MS results imply that although the dimers may form in solution, the $\{Ag_8\}$ ring is assembled only upon crystallization. Therefore, we postulate that the crystal packing requirements of the TBDMS groups and nitrate anions orient the dimers so that $Ag\cdots Ag$ bond formation can occur.

When samples of the $\{Ag_8\}$ cluster were kept dissolved in methanol for several days, a pronounced color change to red was observed. Repeat measurement of the UV spectrum revealed a new peak at around 430 nm, which is consistent with the plasmon absorption of silver nanoparticles.⁴⁰ This color change and UV-vis peak were not observed in samples of **3**, the DAMC-silver(I) nitrate dimer, which were kept for a similar period. Therefore, it appears that the DATC ligand is somehow able to assist in the synthesis of silver nanoparticles, possibly because when DATC is coordinated to the nanoparticle surface, the lipophilic tail is able to exert some control over aggregation processes, in a fashion similar to that of adsorbed surfactant molecules in reverse-micelle-based nanoparticle synthesis.⁴¹

Complexation of DATC with silver(I) perchlorate underlines the importance of the nitrate counterion, in addition to the TBDMS tail group, in formation of **4**. This resulted in crystallization of the helical 1D coordination polymer $[\{Ag(DAHC)\}_n](ClO_4)_n$, **5**, in a 42% yield. In **5**, two-coordinate, linear $Ag(I)$ centers are connected by DATC ligands acting as μ_2 bridges (Figure 5). The silver-nitrogen bond lengths are 2.140(6) and 2.142(5) Å, with a N-Ag-N angle of $175.0(2)^\circ$ indicating the near perfect linearity of the silver coordination environment, see Figure 7. In the crystal, the

(40) Lu, H. W.; Liu, S. H.; Wang, X. L.; Qian, X. F.; Yin, J.; Zhu, Z. K. *Mater. Chem. Phys.* **2003**, *81*, 104. Plyuto, Y.; Berquier, J. M.; Jacquiod, C.; Ricolleau, C. *Chem. Commun.* **1999**, 1653.

(41) Vaucher, S.; Fielden, J.; Li, M.; Dujardin, E.; Mann, S. *Nano Lett.* **2002**, *2*, 225.

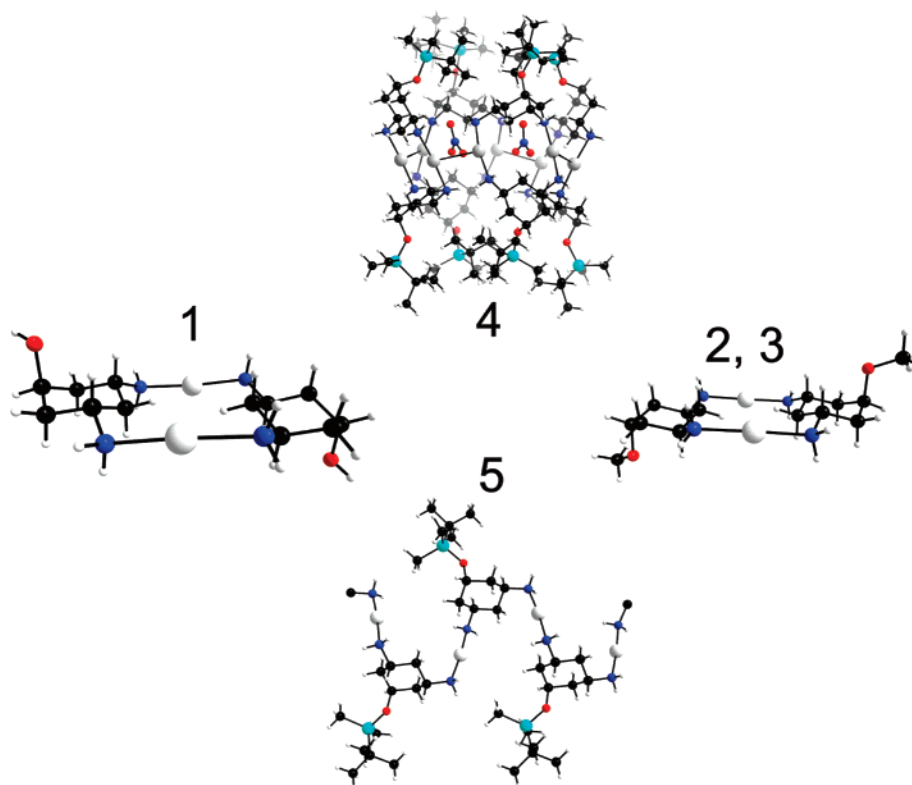


Figure 8. Summary of the structure types formed with the different ligands and anions: Compounds: **1** = DAHC + $(\text{CF}_3\text{SO}_3)_2$; **2** = DAMC + $(\text{CF}_3\text{SO}_3)_2$; **3** = DAMC + NO_3^- - all $\{\text{Ag}_2\}$; **4** = DATC $\{\text{Ag}_8\}$, DAHC + NO_3^- ; **5** = DATC + ClO_4^- $\{\text{Ag}_n\}$.

chains propagate parallel to the crystallographic *b*-axis, with perchlorate counterions aligned on either side of the chains. The shortest perchlorate- $\text{O}\cdots\text{ligand-N}$ distance of approximately 3.11 Å is greater than the sum of the Van der Waal radii, indicating at most a weak contribution from hydrogen bonding, while the interpenetrating arrangement of the TBDMS groups suggests that hydrophobic interactions play a significant role in association of the chains in the crystal. Furthermore, this interpenetrating arrangement appears to be responsible for the helicity of the polymer, because in the analogous structure formed with *cis*-3,5-diaminocyclohexane (e.g., an identical donor set with no hydrophobic “tail” group attached), the arrangement of the silver centers is perfectly linear.²⁵

Summary and Conclusions

In conclusion, this study shows how changes to noncoordinating ligand groups, with retention of the same donor set and topology, can significantly affect the solid-state supramolecular architectures formed. Specifically, addition of the bulky, hydrophobic TBDMS group causes assembly of simple Ag_2L_2 dimers into an $\{\text{Ag}_8\}$ aggregate via $\text{Ag}\cdots\text{Ag}$ interactions, and also imparts a helical twist to a polymeric structure, see Figure 8. Furthermore, it appears that the TBDMS derivatized ligand may be able to direct assembly of silver nanoparticles as well as clusters. Naturally, the influence of the noncoordinating substituent is exerted through secondary noncovalent interactions and the crystal packing requirements of a sterically demanding group and, combined with variations of anion, offers a method to

generate diverse, yet related new structures. Such structures may provide fundamental insight into the self-assembly process: in this case, use of DOSY ^1H NMR and DFT calculations has demonstrated that although $\text{Ag}-\text{Ag}$ bonding may be reasonably strong in the solid state, it is unable to support a large aggregate upon dissolution in polar solvents. In further work, we will continue investigating the solution chemistry of the $\{\text{Ag}_8\}$ aggregate, with a view to finding conditions in which it is stable and potentially capable of acting as a receptor, and carry out a detailed study of the nanoparticle formation that appears to occur in this system. We will also investigate the use of other silyl ethers as tail groups, such as the *O-tert*-butyldiphenylsilyl (TBDPS) group, which in addition to offering greater stability have even greater steric bulk than the TBDMS group.

Acknowledgment. We thank Robert D. Scott of Iowa State University for valuable help with NMR spectroscopy and Andrew Pitt of the University of Glasgow for help with electrospray mass spectrometry. We thank the EPSRC and the Leverhulme Trust for funding. Ames Laboratory is operated for the U.S. Department of Energy by Iowa State University under Contract W-7405-Eng-82.

Supporting Information Available: Crystallographic information for compounds **1–5** in CIF format and supplementary NMR DOSY data (PDF). This material is available free of charge via the Internet at <http://pubs.acs.org>.

IC700872B